Coherent and incoherent pairing instabilities and spin-charge separation in bipartite and nonbipartite nanoclusters: Exact results

A. N. Kocharian,[1] G. W. Fernando,[2] K. Palandage,[2] and J. W. Davenport[3]
[1]*Physics Department, California State University, Los Angeles, California 90032, USA and Physics Department, LACCD Pierce College, Woodland Hills, California 91371, USA*
[2]*U-46, Physics Department, University of Connecticut, Storrs, Connecticut 06269, USA*
[3]*Computational Science Center and Center for Functional Nanomaterials, Brookhaven National Laboratory, Upton, New York 11973, USA*

(Received 5 March 2008; revised manuscript received 4 June 2008; published 21 August 2008)

Electron pairing and formation of various types of magnetic correlations for ensembles of small clusters of different geometries are studied with emphasis on tetrahedrons and square pyramids under variation of interaction strength, electron doping and temperature. These exact calculations of charge and spin collective excitations and pseudogaps yield intriguing insights into level crossing degeneracies, phase separation and condensation. Obtained coherent and incoherent pairings provide a route for possible superconductivity different from the conventional BCS theory. Criteria for spin-charge separation, reconciliation and recombination driven by interaction strength, next-nearest coupling and temperature are found. Resulting phase diagrams resemble a number of inhomogeneous, coherent and incoherent nanoscale phases seen recently in high-T_c cuprates, manganites and colossal magnetoresistive (CMR) nanomaterials.

DOI: 10.1103/PhysRevB.78.075431 PACS number(s): 71.10.Fd, 65.80.+n, 73.22.−f, 71.27.+a

I. INTRODUCTION

Systems with correlated electrons display a rich variety of physical phenomena and properties: different types of magnetic ordering, (high-T_c) superconductivity, ferroelectricity, spin-charge separation, formation of spatial inhomogeneities[1–6] (phase separation, stripes, local gap and incoherent pairing, charge and spin pseudogaps). The realization of these properties in clusters and bulk depends on the interaction strength U, doping, temperature, the detailed type of crystal lattice and sign of coupling t.[7] In addition, studies of perplexing physics of electron behavior in nonbipartite lattices have encountered enormous difficulties. In particular, exact solutions at finite temperatures exist only in a very few cases;[8–10] perturbation theory is usually inadequate while numerical methods have serious limitations, such as in the quantum Monte Carlo method and its notorious sign problem. On the contrary, one can get important insights from the exact solutions for small clusters ("molecules"). For example, squares or cubes are the building blocks, or prototypes, of solids with bipartite lattices, whereas triangles, tetrahedrons, octahedrons without electron-hole symmetry may be regarded as primitive units of typical frustrated systems (triangular, pyrochlore, perovskite). Exact studies of various cluster topologies can thus be very useful for understanding nanoparticles and respective bulk systems.

One can take a further step and consider a bulk system as a collection of many such decoupled clusters, which do not interact directly, but form a system in thermodynamic equilibrium.[10–12] Of course this approach, being perfectly suitable for real systems consisting of nanoclusters, has certain limitations when applied to bulk solids since coupling between such building blocks, in principle, has to be taken into account. The method of decoupled clusters can be approximate for concentrated magnetic and superconducting materials, where coupling between clusters c is comparable to the relevant energy scale within individual clusters, t. However, for inhomogeneous concentrated systems this description in thermodynamic equilibrium becomes quite accurate for suitable values of parameters since the lattice can be broken up into periodic arrays of weakly coupled clusters.[13,14] For example, the tendency to pairing, which can be observed on the example of isolated clusters in thermodynamic equilibrium, is preserved for respective values of parameters also for concentrated systems. On the other hand, the study of small clusters allows us to unravel important details which depend on the local geometry, to investigate the specific features of inhomogeneous, frustrated systems when studying corresponding clusters (triangles, tetrahedrons) as compared with bipartite systems (consisting of building blocks such as dimers or squares). This approach allows us to learn important lessons not only about isolated clusters (for which it is exact), but also about respective spatially inhomogeneous solid materials. This is one of the main aims of the present paper. Thus, we consider a collection of such "clusters" either at a fixed average number of electrons per cluster in a canonical ensemble or for a fixed chemical potential μ in a grand canonical ensemble.

When correlations are local, many physical phenomena observed in "large" concentrated systems are also clearly seen in our examples of small clusters in thermodynamic equilibrium; in addition, our studies have the advantage of being exact. We will demonstrate that already at this level it is possible to observe phenomena such as spin-charge separation, formation of states with charge and spin pseudogaps due to electron pairing, formation of different magnetic states, etc. The electrons can be splintered apart by spin-charge separation due to level crossings driven by U or temperature, so that the collective excitations of electron charge and spin of different symmetries can become quite independent and propagate incoherently. We have found that local charge and spin density of states or corresponding suscepti-

bilities can have different pseudogaps which is a sign of spin-charge separation. For large U near half filling, holes prefer to be localized on separate clusters having Mott-Hubbard (MH)-type charge pseudogaps[12] and Nagaoka ferromagnetism (FM);[7] otherwise, spin density waves or spin liquids may be formed. At moderate U, this approach leads to recombination of charge and spin degrees with redistribution of charge carriers or holes between square clusters. The latter, if present, can signal a tendency toward phase separation, or, if clusters "prefer" to have two holes, it can be taken as a signature of pairing.[13] This, in turn, could imply imposed opposite spin pairing followed by condensation of charge and spin degrees into a BCS-type coherent state. Although this approach for large systems is only approximate, it nonetheless gives very important clues for understanding large systems whenever correlations are local.

We have developed this approach in Refs. 11, 12, and 15–17 and successfully applied it to typical unfrustrated (linked squares) clusters. Our results are directly applicable to nanosystems which usually contain many clusters, rather well separated and isolated from each other but nevertheless being in thermodynamic equilibrium with the possibility of having spatial inhomogeneities for different numbers of electrons per cluster. Interestingly, an ensemble of square clusters displays "checkerboard" patterns, nanophase inhomogeneity, incoherent pairing and nucleation of pseudogaps.[1–5] The purpose of this work is to further conduct similar extensive investigations in frustrated systems,[18] exemplified by four-site tetrahedrons and five-site square pyramids. The exact studies here of phase diagrams using canonical and grand canonical ensemble calculations in finite-size clusters having immediate applications to nanosystems can motivate further studies of electronic and magnetic instabilities in Nb, Co nanoclusters, and clusters of correlated materials. As we shall see, certain features in contrasting topologies are quite different and these predictions could be exploited in the nanoscience frontier by synthesizing clusters or nanomaterials with unique properties.[19]

II. MODEL AND FORMALISM

We model our systems by the Hubbard model,

$$H = -t\sum_{\langle ij\rangle\sigma} c^{+}_{i\sigma}c_{j\sigma} + U\sum_{i} n_{i\uparrow}n_{i\downarrow}. \quad (1)$$

Our approach is to use the exact diagonalization for finite clusters of a certain type, and then considering the ensemble of such clusters by calculating the canonical and grand partition functions, thermodynamic potentials, and, most importantly, response functions such as the charge χ_c and spin χ_s susceptibilities, i.e., *fluctuations*. For fixed T and U we calculate the energy differences $\mu_+ = E(N+1) - E(N)$ and $\mu_- = E(N) - E(N-1)$ for average canonical energies $E(N)$ by adding or subtracting one electron (charge) with various configurations of electrons for given spin S. The charge energy gap at finite temperature can be written as $\Delta^c(T) = \mu_+ - \mu_- = E(N+1) + E(N-1) - 2E(N)$. We calculate also a spin gap $\Delta^s(T) = E(S+1) - E(S)$ for $E(S)$ being respectively the average canonical energy in spin sector at fixed N. The charge and spin energy gaps as shown in Ref. 12 can be considered as natural order parameters in multidimensional parameter space T, U, μ, h and at $T \neq 0$ are called *pseudogaps*, since χ has a small, but nonzero weight inside the gap. Thus we define critical U and intercluster coupling c parameters for level crossings degeneracies or quantum critical points from condition at which charge or spin pseudogaps are vanished, $\Delta^{c,s}(U,c) = 0$. The pseudogap sign is also important in identifying the regions for electron charge and spin instabilities, such as electron-electron ($\Delta^c < 0$), electron-hole ($\Delta^c > 0$) pairings in charge sector or parallel ($\Delta^s < 0$) and opposite ($\Delta^s > 0$) spin pairings in spin sector. The negative pseudogaps describe possible hole or parallel spin pairs binding instabilities. For charge degrees this is a sign toward phase separation (*i.e., segregation*) of clusters on hole-rich (charge neutral) and hole-poor regions. In contrast, negative spin pairing gap for parallel spins reveals domain structure and ferromagnetism in accordance with Nagaoka theorem. Therefore, one can introduce also corresponding crossover temperatures T_c^P, T_c, T_s^P and T_s^F versus chemical potential using condition $\Delta^{c,s}(T,\mu) = 0$ at which the corresponding pseudogaps for those various phases disappear. In addition, the pseudogap parameters for various transitions, corresponding phase boundaries and crossover temperatures can be found by monitoring maxima and minima in charge and spin susceptibilities. At low temperature, peak structures in $\chi_c(\mu)$ and zero magnetic field spin susceptibility, $\chi_s(\mu)$, are observed to develop in these clusters; between two consecutive peaks, there exists a pseudogap in charge or spin degrees. The opening of such distinct and separated pseudogap regions for spin and charge degrees of freedom (at low temperature) is a signature of corresponding charge and spin separation away from half filling. However, at a certain parameter range, the charge and spin susceptibilities can closely follow each other which shows the tendency of electron spin and charge toward recombination and reconciliation.

Below in Secs. III A and III B, we study nodes, sign and amplitude of charge and spin gaps that provide valuable insights into quantum critical points and various phase transitions. By monitoring the susceptibility peak positions in χ^c and χ^s and pseudogaps as a function of temperature and chemical potential, one can identify relevant crossover temperatures that have been used to construct the phase diagrams in Sec. III C.

III. RESULTS

A. Bipartite clusters

For completeness and to facilitate the comparison with frustrated clusters, we first summarize the main results obtained earlier for small 2×2 and 2×4-sites bipartite clusters in Refs. 11, 12, 15, and 16. The energies are measured in units $|t| = 1$ in all results that follow. Figure 1 illustrates Δ^c and Δ^s in ensemble of 2×2 square clusters at $\langle N\rangle \approx 3$ and $T \to 0$. Vanishing of gaps indicates energy (multiple) level crossings and corresponding quantum critical points, U_c and U_F. The negative gaps show phase separations for charge below $U_c = 4.584$ and spin degrees above $U_F = 18.583$.[10,11]

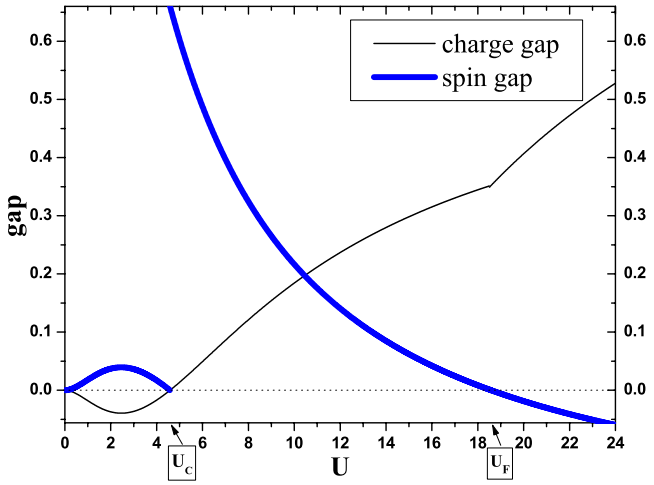

FIG. 1. (Color online) Charge Δ^c and spin Δ^s gaps versus U in an ensemble of squares at $\langle N\rangle \approx 3$ and $T=0$. Phase A: Charge and spin pairing gaps of equal amplitude at $U \leq U_c$ describe Bose condensation of electrons similar to BCS-type coherent pairing with a single energy gap. Phase B: Mott-Hubbard-type insulator at $U_c < U < U_F$ leads to $S=\frac{1}{2}$ spin liquid behavior. Phase C: Parallel (triplet) spin pairing ($\Delta^s < 0$) at $U > U_F$ displays $S=\frac{3}{2}$ saturated ferromagnetism (see Sec. III A). The spin gap in Phase A for $U \leq U_c$ region has been derived in grand canonical approach for very low temperatures ($T \to 0$).

Phase A: Negative charge gap below U_c displays electron pairing $\Delta^P = |\Delta^c|$ and charge phase separation into hole-rich (charged) metal and hole-poor (neutral) cluster configurations. In a grand canonical approach $\Delta^s > 0$ at $U \leq U_c$ corresponds to electron charge redistribution with opposite spin (singlet) pairing. This picture for electron charge and spin gaps of equal amplitude $\Delta^s \equiv \Delta^P = -\Delta^c$ of purely electronic nature at $\langle N\rangle \approx 3$ is similar to the BCS-type coherency in the attractive HM and will be called coherent pairing (CP). In equilibrium, the spin singlet background ($\chi_s > 0$) stabilizes phase separation of paired electron charge in quantum CP phase. The unique gap $\Delta^s \equiv \Delta^P$ at $T=0$ in Fig. 1 is consistent with the existence of a single quasiparticle energy gap in the BCS theory for $U < 0$.[20] Positive spin gap in Fig. 1 at $U < U_c$ provides pair rigidity in response to a magnetic field and temperature (see Sec. III C). However, unlike in the BCS theory, the charge gap differs from spin gap as temperature increases. This shows that coherent thermal excitations in the exact solution are not quasiparticle-like renormalized electrons, as in the BCS theory, but collective paired charge and coupled opposite spins. We find also rigorous conditions in inhomogeneous systems for redistribution of electron spin between clusters, when due to the charge and spin separation at large U it is energetically favorable for two parallel spins to arrive on one cluster while holes can stay localized on each of these two clusters. The negative spin gap $\Delta^s < 0$ for excited $S=\frac{3}{2}$ configuration in Fig. 1 above U_c is shown for canonical energies in a stable MH-type state, $\Delta^c > 0$. Phase B: Unsaturated ferromagnetism (UF) for unpaired $S=\frac{1}{2}$ with zero field χ^s peak for gapless $s_z = \pm\frac{1}{2}$ projections and gapped $\Delta^s > 0$ for $S=\frac{3}{2}$ excitations at $U_c \leq U \leq U_F$ will be called a spin liquid. Phase C: Negative $\Delta^s < 0$ at $U > U_F$ defines $S = \frac{3}{2}$ saturated ferromagnetism (SF). Localized holes at $\Delta^c > 0$ rule out possible Nagaoka FM in a metallic ground state (GS).[7] Field fluctuations lift s_z-degeneracy and lead to segregation of clusters into magnetic domains.

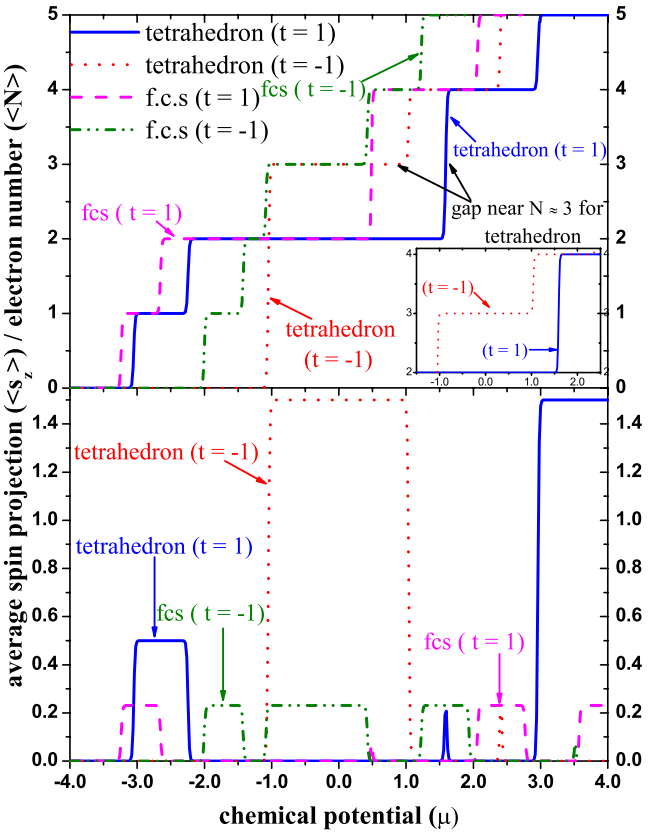

FIG. 2. (Color online) $\langle N\rangle$ and $\langle s^z\rangle$ versus μ in grand canonical ensemble of tetrahedrons and fcs at $U=4.0$, $T=0.01$ and $h=0.1$. Mott-Hubbard-type ferromagnetism for $\langle s_z\rangle = \frac{3}{2}$ at $\langle N\rangle = 3$ in tetrahedron occurs for $t=-1$, while absence of charge pseudogap near $\langle N\rangle \approx 3$ metallic state with spin rigidity manifests level crossing degeneracy related to pairing (see inset).

We have found that the ensemble of squares share common important features with the large bipartite clusters in the ground state and at finite temperatures[20,21] (see also Sec. III C). Previously, for 2×4 ladders we did report in Fig. 5 of Ref. 16 an oscillatory behavior of charge gap ($T=0$) as a function of U. As for squares at low temperatures, we observe similar level crossing degeneracies in charge and spin sectors also in bipartite 2×4 clusters at relatively small and large U values, respectively. Thus the use of chemical potential and departure from zero-temperature singularities in canonical and grand canonical ensembles appear to be essential for understanding important physics related to the pseudogaps, phase separation, pairings and corresponding crossover temperatures. A full picture of coherent and incoherent pairing, electronic inhomogeneities and magnetism emerges only at finite, but rather low temperatures. (If we set $t=1$ eV, most of the interesting physics is seen to occur below a few hundred degrees K.)

B. Tetrahedrons and square pyramids

The topology of the tetrahedron is equivalent to a square with next-nearest-neighbor coupling ($t' = t$) while the square

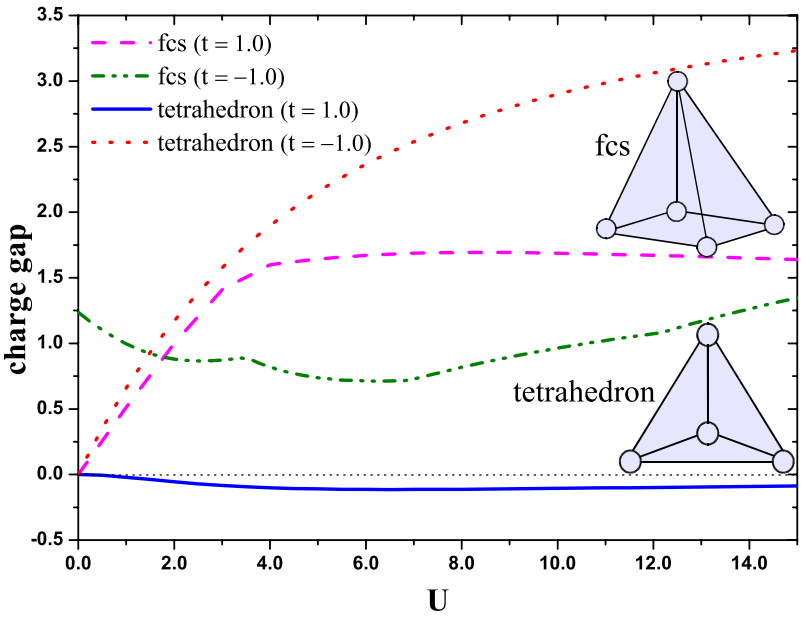

FIG. 3. (Color online) Δ^c versus U for one hole off half filling in tetrahedrons and fcs at $T=0$. In tetrahedron, $\Delta^c<0$ at $t=1$ implies phase separation and coherent pairing with $\Delta^s \equiv \Delta^P$, while $\Delta^c>0$ for $S=\frac{3}{2}$ at $t=-1$ leads to a ferromagnetic insulator ($\Delta^s<0$) for all U. In fcs, $\Delta^c>0$ at $\langle N\rangle \approx 4$ for $t=\pm 1$ describes Mott-Hubbard-type antiferromagnetism ($\Delta^s>0$).

pyramid of the octahedral structure in high-T_c superconductors (HTSCs) is related to face-centered squares (fcs). The average electron number $\langle N\rangle$ and magnetization $\langle s^z\rangle$ versus μ in Fig. 2 for $T=0.01$ shows contrasting behavior in pairing and magnetism at $t=1$ and $t=-1$ for the tetrahedron at $\langle N\rangle=3$ and fcs at $\langle N\rangle=4$. Different signs of t in these topologies for one hole off half filling lead to dramatic changes in the electronic structure. Figure 3 illustrates the charge gaps at small and moderate U. Tetrahedron at $t=-1$: SF with a negative spin gap in a MH-type phase exists for all U. Tetrahedron at $t=1$: metallic CP phase with charge and spin gaps of equal amplitudes similar to the BCS-type pairing, discussed for squares in Sec. III A, is formed at all U. FCS at $t=-1$: MH-type insulator displays two consecutive crossovers at $U\simeq 6.89$ from ($S=0$) antiferromagnetism (AF) into ($S=1$) UF and into ($S=2$) SF above $U=12.19$. FCS at $t=1$: MH-type insulator shows crossover at $U\simeq 29.85$ from ($S=0$) AF into ($S=1$) UF. In triangles, SF and AF are found to be stable for all $U>0$ at $t=-1$ and $t=1$, respectively. Finally Table I illustrates magnetic phases at large U and $T=0$. For example, the squares and all frustrated clusters at $t=-1$ exhibit stable SF; tetrahedron and triangle at $t=1$ retain CP and AF, respectively; UF for the $S=1$ state, separated by $\Delta^s=-0.115$ from $S=0$, exists in fcs at $t=1$. Figure 4 shows charge gap at two coupling values c between the vertex and base atoms in the deformed tetrahedron. Vanishing of the gap, driven by c, manifests level crossings for $c=0.96$, while $c=1.1$ and $t=1$ cases describe a single phase with avoided crossings.

C. Phase diagrams

Figure 5 illustrates a number of nanophases, defined in Refs. 12 and 16, for the tetrahedron similar to bipartite clusters. The curve $\mu_+(T)$ below T_c^P signifies the onset of charge paired condensation. As temperature is lowered below T^*, a spin pseudogap is opened up first, as seen in NMR experiments,[16] followed by the gradual disappearance of the spin excitations, consistent with the suppression of low-energy excitations in the HTSCs probed by STM.[3–5] The opposite spin CP phase with fully gapped collective excitations begins to form at $T\leq T_s^P$. The charge inhomogeneities[1,2] of hole-rich and charge neutral *spinodal* regions between μ_+ and μ_- are similar to those found in the squares and resemble important features seen in the HTSCs. Figure 5 shows the presence of bosonic modes below $\mu_+(T)$ and T_s^P for paired electron charge and opposite spin, respectively. This picture suggests condensation of electron charge and spin at various crossover temperatures while condensation in the BCS

TABLE I. GS in various cluster geometries for one hole off half filling at large $U=900$ and $t=\pm 1$ having saturated ferromagnetism (SF), unsaturated ferromagnetism (UF), antiferromagnetism (AF), or coherent pairing (CP).

Cluster type	N_a	N	S	Δ^s	Δ^c	t	GS
Triangle	3	2	1	−0.998	3.093	−1	SF
Tetrahedron/nnn square	4	3	1.5	−0.997	3.987	−1	SF
Square pyramid/fcs	5	4	2	−0.417	2.596	−1	SF
Square	4	3	1.5	−0.262	1.15	±1	SF
Triangle	3	2	0	1.008	2.011	1	AF
Tetrahedron/nnn square	4	3	0	0.002	−0.002	1	CP
Square pyramid/fcs	5	4	1	−0.115	1.543	1	UF

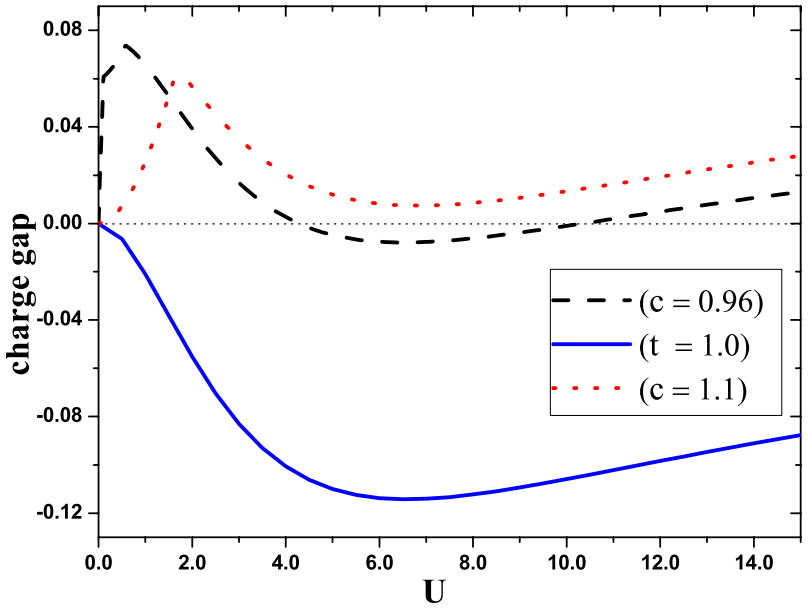

FIG. 4. (Color online) Δ^c versus U at $\langle N\rangle=3$ and $T=0.01$ in tetrahedron ($t=1$) and deformed tetrahedral clusters ($c=0.96$ and 1.1). Charge and spin pairing gaps of equal amplitude at $t=1$ imply coherent pairing, while $\Delta^c>0$ and $\Delta^s<0$ at $c=1.1$ correspond to an unsaturated ferromagnetic insulator for $S=\frac{1}{2}$. Coherent pairing is retained in a narrow range near $c\approx 1$.

theory occurs at a single T_c value. The temperature driven spin-charge separation above T_s^P resembles an incoherent pairing (IP) phase seen in the HTSCs.[2–5] The charged pairs without spin rigidity above T_s^P, instead of becoming superconducting, coexist in a nonuniform, charge degenerate IP state similar to a ferroelectric phase.[20,21] The unpaired weak moment, induced by a field above T_s^P, agrees with the observation of competing dormant magnetic states in the HTSCs.[4] The coinciding χ^s and χ^c peaks at $T_s^P\leq T\leq T'$ show full reconciliation of charge and spin degrees seen in the HTSCs above T_c. In the absence of electron-hole symmetry, the tetrahedral clusters near optimal doping μ_P undergo a thermal transition from a CP phase into a MH-type phase.

IV. CONCLUSION

Our exact calculations, ideally suited for real nanosystems consisting of weakly coupled clusters, have certain limitations when applied to bulk solids with relatively strong coupling between clusters. Although approximate for large systems, it provides a parameter window for understanding important ground state and thermal properties of correspond-

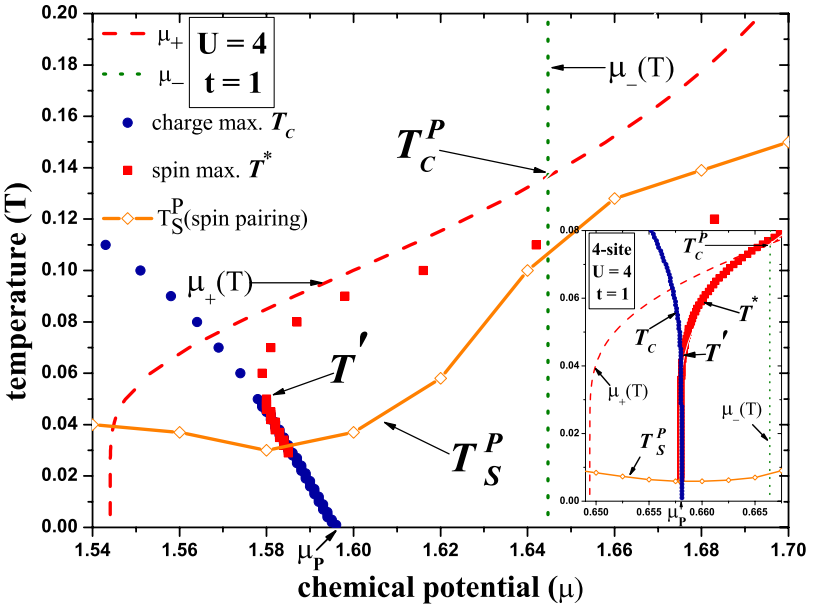

FIG. 5. (Color online) The T-μ phase diagram of tetrahedrons without electron-hole symmetry at optimally doped $\langle N\rangle\approx 3$ regime near $\mu_P=1.593$ at $U=4$ and $t=1$ illustrates the condensation of electron charge and onset of phase separation for charge degrees below T_c^P. The incoherent phase of preformed pairs with unpaired opposite spins exists above T_s^P. Below T_s^P, the paired spin and charge coexist in a coherent pairing phase. The charge and spin susceptibility peaks, denoted by T^* and T_c, define pseudogaps calculated in the grand canonical ensemble, while $\mu_+(T)$ and $\mu_-(T)$ are evaluated in canonical ensemble. Charge and spin peaks reconcile at $T'\geq T\geq T_s^P$, while χ^c peak below T_s^P signifies metallic (charge) liquid (see inset for square cluster and Ref. 16).

ing large systems. The collection of weakly coupled arrays of clusters gives valuable clues for understanding the thermodynamic perplexities of inhomogeneous, concentrated systems. Many complex phenomena, apparent in approximate treatments of "large" inhomogeneous systems, are also observed in our exact studies of phase diagrams for ensemble of small clusters, which do interact thermally.[21] Already at this level, we can see such phenomena as level crossings, spin-charge separation, similar charge (hole) or parallel spin pairings, charge and spin pseudogaps that are preserved for respective values of parameters in concentrated (bulk) systems. A collection of clusters seems to yield an adequate thermodynamic description of pairing instabilities in inhomogeneous structures that can be useful for understanding the mechanism of superconductivity and magnetism at the nanoscale when correlations are local. The experimental observations of spatial inhomogeneities, incoherent pairing and pseudogaps in HTSCs and various (magnetic) manganites give strong support in this regard. Thus it is clear that our exact results provide insight into level crossings, spin-charge separation, reconciliation (recombination) and full Bose condensation.[22] Moreover, the separate condensation of electron charge and spin degrees offers a new route to superconductivity in inhomogeneous HTSC systems, different from the BCS scenario. The electronic instabilities found for various geometries, in a wide range of U, coupling c and temperatures, will be useful for the prediction of electron pairing, ferroelectricity[20,21] and possible superconductivity in nanoparticles, doped cuprates, etc.[1–6]

In addition, these exact studies of the local geometry at $t=\pm 1$ of parameter t in isolated clusters (for which it is exact) reveal important similarities and differences for corresponding large systems consisting of these "primitive" bipartite and frustrated blocks. For example at $t=1$, in contrast to the bipartite clusters, exact solutions for the tetrahedron clusters exhibit coherent and incoherent pairings for all U. However at $t=-1$, the tetrahedral clusters can facilitate Nagaoka-type saturated ferromagnetism for all $U>0$ that can explain pressure and doping dependencies of ferromagnetic transition temperature in concentrated pyrochlores, $A_2Mn_2O_7$ (A = Y, In, Lu, and Tl).[23] Our findings of various magnetic instabilities at small, moderate and large U carry a wealth of new information at finite temperatures related to phase separation, saturated ferromagnetism and Nagaoka instabilities in manganites/CMR materials. We find that one can produce electronic and magnetic instabilities in nanoclusters by tuning also intracluster coupling in various topologies of correlated materials. These exact calculations illustrate important clues and exciting opportunities that could be utilized when synthesizing potentially high-T_c superconducting and magnetic nanoclusters assembled in two- and three-dimensional geometries.[19] Ultracold fermionic atoms in an optical lattice[24] may also offer unprecedented opportunities to test these predictions.

Note added in proof. Recently, we found that some of our previous exact results in Refs. 11 and 12 and charge pairing gaps in larger 2×4 clusters[15,16] have been reproduced for the ground state by others later in Ref. 25. However, as we notice the departure from the ground state to finite temperatures is crucial for understanding in nanoscale level the effect of coherent and incoherent pairings, spin-charge separation, recombination (reconciliation) and full Bose condensation, formation of MH-type behavior and spin pseudogaps, magnetic crossover temperatures, etc. in HTSCs, manganites and other transition metal oxides.

ACKNOWLEDGMENTS

We thank Daniil Khomskii and Valery Pokrovsky for helpful discussions and Tun Wang for valuable contributions. This research was supported in part by U.S. Department of Energy under Contract No. DE-AC02-98CH10886.

[1] Y. Kohsaka, C. Taylor, K. Fujita, A. Schmidt, C. Lupien, T. Hanaguri, M. Azuma, M. Takano, H. Eisaki, H. Takagi, S. Uchida, and J. C. Davis, Science **315**, 1380 (2007).
[2] T. Valla, A. V. Fedorov, Jinho Lee, J. C. Davis, and G. D. Gu, Science **314**, 1914 (2006).
[3] A. C. Bódi, R. Laiho, and E. Lähderanta, Physica C **411**, 107 (2004).
[4] H. E. Mohottala, B. O. Wells, J. I. Budnick, W. A. Hines, C. Niedermayer, L. Udby, C. Bernard, A. R. Moodenbaugh, and F. C. Chou, Nat. Mater. **5**, 377 (2006).
[5] K. K. Gomes, A. N. Pasupathy, A. Pushp, S. Ono, Y. Ando, and A. Yazdani, Nature (London) **447**, 569 (2007).
[6] R. Moro, S. Yin, X. Xu, and W. A. de Heer, Phys. Rev. Lett. **93**, 086803 (2004); X. Xu, S. Yin, R. Moro, and W. A. de Heer, *ibid.* **95**, 237209 (2005).
[7] Y. Nagaoka, Phys. Rev. **147**, 392 (1966).
[8] H. Shiba and P. A. Pincus, Phys. Rev. B **5**, 1966 (1972).
[9] L. M. Falicov and R. H. Victora, Phys. Rev. B **30**, 1695 (1984).
[10] R. Schumann, Ann. Phys. (N.Y.) **11**, 49 (2002); **17**, 64 (2008).
[11] A. N. Kocharian, G. W. Fernando, K. Palandage, and J. W. Davenport, J. Magn. Magn. Mater. **300**, e585 (2006).
[12] A. N. Kocharian, G. W. Fernando, K. Palandage, and J. W. Davenport, Phys. Rev. B **74**, 024511 (2006).
[13] W.-F. Tsai and S. A. Kivelson, Phys. Rev. B **73**, 214510 (2006).
[14] L. N. Bulaevskii, C. D. Batista, M. Mostovoy, and D. Khomskii, Phys. Rev. B **78**, 024402 (2008).
[15] A. N. Kocharian, G. W. Fernando, K. Palandage, and J. W. Davenport, Phys. Lett. A **364**, 57 (2007).
[16] G. W. Fernando, A. N. Kocharian, K. Palandage, Tun Wang, and J. W. Davenport, Phys. Rev. B **75**, 085109 (2007).
[17] K. Palandage, G. W. Fernando, A. N. Kocharian, and J. W. Davenport, J. Comput.-Aided Mater. Des. **14**, 103 (2007).
[18] I. A. Sergienko and S. H. Curnoe, Phys. Rev. B **70**, 144522 (2004).
[19] S. Y. Wang, J. Z. Yu, H. Mizuseki, Q. Sun, C. Y. Wang, and Y. Kawazoe, Phys. Rev. B **70**, 165413 (2004).
[20] A. N. Kocharian, G. W. Fernando, K. Palandage, and J. W. Davenport, in MISM Conference Proceedings, Material Science Fo-

rum, Moscow, 2008.
[21] A. N. Kocharian, G. W. Fernando, K. Palandage, and J. W. Davenport, arXiv:0804.0958 (unpublished).
[22] R. Friedberg, T. D. Lee, and H. C. Ren, Phys. Rev. B **50**, 10190 (1994).
[23] Y. Shimakawa, Y. Kubo, and T. Manako, Nature (London) **379**, 53 (1996).
[24] J. K. Chin, D. E. Miller, Y. Liu, C. Stan, W. Setiawan, C. Sanner, K. Xu, and W. Ketterle, Nature (London) **443**, 961 (2006).
[25] W.-F. Tsai, H. Yao, A. Läuchli, and S. A. Kivelson, Phys. Rev. B **77**, 214502 (2008).